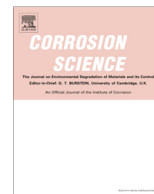




Contents lists available at ScienceDirect

## Corrosion Science

journal homepage: [www.elsevier.com/locate/corsci](http://www.elsevier.com/locate/corsci)

## Effect of sealing on the morphology of anodized aluminum oxide

Naiping Hu<sup>a</sup>, Xuecheng Dong<sup>a</sup>, Xueying He<sup>a</sup>, James F. Browning<sup>b</sup>, Dale W. Schaefer<sup>a,\*</sup><sup>a</sup> Department of Biomedical, Chemical and Environmental Engineering, College of Engineering and Applied Science, University of Cincinnati, Cincinnati, OH 45221-0012, USA<sup>b</sup> Spallation Neutron Source, Oak Ridge National Laboratories, Oak Ridge, TN 37831, USA

## ARTICLE INFO

## Article history:

Received 20 September 2014

Accepted 8 March 2015

Available online xxxxx

## Keywords:

- A. Aluminum
- B. X-ray diffraction
- B. EIS
- B. Reflectivity
- C. Anodic films
- C. Interfaces

## ABSTRACT

Ultra-small angle X-ray scattering (USAXS), small-angle neutron scattering (SANS), X-ray reflectometry (XRR) and neutron reflectometry (NR) were used to probe structure evolution induced by sealing of anodized aluminum. While cold nickel acetate sealing and hot-water sealing decrease pore size, these methods do not alter the cylindrical porous framework of the anodic aluminum oxide layer. Hot nickel acetate both fills the pores and deposits on the air surface (air–oxide interface), leading to low porosity and small mean pore radius (39 Å). Electrochemical impedance spectroscopy and direct current polarization show that samples sealed by hot nickel acetate outperform samples sealed by other sealing methods.

© 2015 Elsevier Ltd. All rights reserved.

## 1. Introduction

Anodized aluminum displays an unusual porous structure. It is widely accepted that the anodizing film has a two-layer structure – a nonporous barrier oxide and a porous outer oxide. The thin barrier layer (10–100 nm) is found at the bottom of the pores at the metal interface [1–5]. The porous anodized aluminum oxide (AAO) structure is reported to be an ordered hexagonal array of cells with cylindrical pores of diameter 25 nm to 0.3 μm and depths exceeding 100 μm [6,7]. For low-voltage anodization our recent study by neutron/X-ray reflectometry and small-angle scattering confirms the cylindrical pore structure. In addition, scattering data show that the AAO pore diameter and inter-pore spacing are fixed in the first 10 s of anodizing, after which the pores linearly penetrate the aluminum at constant diameter and spacing [8]. A moderately high porosity of 40% was determined by ultra-small angle X-ray scattering (USAXS) analysis, X-ray reflectometry (XRR) and neutron reflectometry (NR).

Due to the porous nature of AAO films, sealing is necessary [9,10] to improve corrosion resistance. Sealing strategies based on various combinations of temperature and sealing bath chemistry all improve corrosion resistance to some extent [10]. Sealing traditionally has been done by immersion in boiling deionized water, a method known as hot water sealing [11–13]. The high temperature required and slow kinetics, however, imply considerable energy consumption [14]. As a result the hot water process

has been gradually superseded since 1980s by cold sealing [12]. Dichromate and nickel acetate sealing are considered the most effective sealing methods for corrosion prevention [10]. However Cr(VI) is recognized as toxic [13,15–17]. A number of sealants have been proposed for sealing applications and new sealing processes are emerging [18].

Recent studies on new sealants and sealing processes include cold nickel acetate sealing [13], sodium silicate sealing [18], nickel fluoride sealing [10,18], Cr<sub>2</sub>O<sub>3</sub> sealing [19], sodium acetate sealing [12,14], cerium acetate sealing [17,20], cerium nitrate and yttrium sulfate sealing [9], sol–gel sealing [16], and even a sealing process using polytetrafluoroethylene (PTFE) [19]. In spite of these efforts to improve the performance, more convenient and effective processes are still needed [19].

In developing the new sealing methods, DC polarization (DCP) [10,19,21,22] and electrochemical impedance spectroscopy (EIS) [13,15–17,20,23–25] have been used to compare the corrosion performance among different methods. For hydrothermal sealing it is believed that boehmite (AlOOH) is produced at temperatures above 80 °C, while hydrargillite (Al(OH)<sub>3</sub>) is formed at low temperatures. For cold sealing methods, however, the mechanism has not been completely elucidated [18]. The structural alternation induced by sealing and the relationship between pore evolution and corrosion resistance have not been investigated.

In this work, we use X-ray reflectivity (XRR), neutron reflectivity (NR), ultra-small-angle X-ray scattering (USAXS) and small-angle neutron scattering (SANS) to investigate the morphological changes induced by sealing. Cold nickel acetate sealing is of particular interest as it has been reported to be a promising alternative to

\* Corresponding author.

E-mail address: [dale.schaefer@uc.edu](mailto:dale.schaefer@uc.edu) (D.W. Schaefer).

conventional hot water sealing [10,13,17,20]. Our results, however, show that both Ni and high temperature are required for effective corrosion protection.

## 2. Materials and methods

### 2.1. Materials

For the electrochemical performance testing, AA1100 coupons (99.00% Al, from ACT, Hillsdale, MI, USA) were used. Each coupon was cut into  $5.08 \times 5.08 \text{ cm} \times 1 \text{ mm}$  panels, polished and rinsed in ethanol. These metal panels provide the optimal dimensions and mechanical strength for our electrochemical measurements. For the USAXS and SANS experiments, we used pure Al foils ( $0.025 \text{ mm} \times 50 \text{ mm} \times 50 \text{ mm}$ , 99.45% Al by Alfa Aesar, MA, USA) to insure X-ray and neutron transmission through the samples.

Both NR and XRR require smooth substrates, accounting for the choice of Al-coated Si wafer substrates. One-side-polished single crystal (111) wafers ( $5.08$  or  $7.62 \text{ cm}$  diameter, and  $5 \text{ mm}$  thickness) were purchased from Wafer World, Inc. (West Palm Beach, FL, USA). A standard cleaning process (Piranha etching followed by ethanol rinsing) was applied on these wafers. Wafers were rinsed until ethanol did not bead up on the silica surface. Then the wafers were dried in  $\text{N}_2$  and stored in sealed container prior to the electron-beam evaporation of the pure Al coating.

### 2.2. Anodizing of Al coupons and foils for USAXS and SANS

In preparation for porous AAO films on AA1100 coupons and pure Al foils, clean samples were dipped in a 20-wt% sulfuric acid at a constant voltage (15 V) controlled by a DC power supply (Instek Test Instrument, San Diego, CA). A graphite counter electrode was used ( $5\text{-mm}$  diameter cylinder). The distance between the graphite cathode and anode was fixed at  $10 \text{ cm}$ . Samples were anodized for maximum time (typically  $120 \text{ min}$  for coupons, and up to  $120 \text{ seconds}$  for Al foils). In the case of the foils, the current drops to zero when the pores fully penetrate. The temperature of anodizing was not controlled. The final samples were air-dried for  $24 \text{ h}$  after cleaning in de-ionized water.

### 2.3. Anodizing on Al-coated Si wafers for XRR and NR

The voltage control method used for the coupons and foils proved to be too aggressive for thin Al layers on Si wafers. Therefore, a current-limited, voltage-controlled protocol was used to obtain suitable AAO films on Al-coated Si wafers. This method modifies the conventional constant-voltage anodizing protocol so that AAO film growth can be controlled [8]. If the measured current density during anodizing is lower than the current limit, the voltage will be maintained at the fixed value. Otherwise, the current density will be controlled at the current density limit. An optimized voltage of  $15 \text{ V}$  and current limit of  $0.015 \text{ A cm}^{-2}$  were identified previously [8] and used in this study. Samples were anodized at  $15 \text{ V}$  and  $0.015 \text{ A cm}^{-2}$  for  $30 \text{ s}$  to reach the maximum AAO thickness without stripping the Al film. These samples were used for XRR and NR studies. As will be described below, these films showed different sealing characteristics compared to the foils formed under voltage-control.

### 2.4. Sealing of anodic aluminum oxide

The AAO films were sealed by four methods: hot water, hot  $5 \text{ g/L}$  nickel acetate, cold  $5 \text{ g/L}$  nickel acetate, and cold saturated nickel acetate ( $180 \text{ g/L}$ ). The hot sealing methods were only used on Al foils and Al coupons because thin coatings on wafers delaminate

at high temperatures. Cold sealing methods were applied on all samples. For hot water and hot nickel acetate sealing, the Al foil/coupon samples were immersed in boiling water ( $100^\circ\text{C}$ ) or hot nickel acetate ( $90^\circ\text{C}$ ) for  $30 \text{ min}$ . For cold sealing, the samples were immersed in nickel acetate solutions for  $30 \text{ min}$  at room temperature.

### 2.5. Ultra-small angle X-ray scattering (USAXS) and small-angle neutron scattering (SANS)

The Al foils were used to prepare the anodized and sealed samples for USAXS and SANS experiments. Foils were anodized up to  $120 \text{ s}$  in 20-wt% sulfuric acid electrolyte at a voltage of  $15 \text{ V}$  without current control. We assume that all the aluminum is converted completely into anodized film at  $120 \text{ s}$  when current drops to zero. The same sealing and cleaning procedure as described for Al coupons was performed on the anodized Al foils.

USAXS was performed at the 15 ID-B beamline at the Advanced Photon Source (APS), Argonne National Laboratories (Argonne, IL, USA). SANS was performed at the Lujan Neutron Scattering Center, Los Alamos National Laboratory (Los Alamos, NM, USA) using the LQD instrument.

In USAXS and SANS, we measure the differential scattering cross section per unit volume on an absolute scale, which is referred to as the intensity,  $I(q)$ , as a function of  $q$ , the magnitude of the momentum transfer. The USAXS and SANS data were first subject to an air background subtraction. The USAXS data then were subject to a unified fit [26] using the APS routines [27]. All USAXS data fitting was done on the slit-smeared data using the appropriate resolution function to smear the calculated model. The pinhole SANS data are not slit-smeared.

### 2.6. X-ray reflectometry (XRR) and neutron reflectometry (NR)

Samples for XRR and NR were prepared by anodizing aluminum films deposited on Si wafers. Reflectometry was used to determine the composition and thickness of deposited thin films. The XRR measurements were carried out on the X'Pert PANalytical X-ray reflectometer at the Advanced Materials Characterization Center at the University of Cincinnati. NR was performed at the Surface Profile Analysis Reflectometer (SPEAR), Lujan Neutron Scattering Center (LANSCE) at Los Alamos National Laboratory (LANL); and the Liquids Reflectometer (LR), Spallation Neutron Source (SNS) at Oak Ridge National Laboratory (ORNL).

In the NR and XRR experiments, a wafer sample is irradiated by the incident beam (neutron or X-ray) at a very small incident angle,  $\theta$ . The ratio of the fluxes of the reflected beam to the incident beam is measured as a function of scattering vector,  $q$ . The relationship between  $\theta$  and  $q$  is:

$$q = \frac{4\pi \sin \theta}{\lambda} \quad (1)$$

where  $\lambda$  is the wavelength of the incident beam. For Cu  $K\alpha$  X-rays,  $\lambda$  is  $1.54 \text{ \AA}$ . For NR,  $\theta$  is fixed and a broad spectrum of wavelengths impinges on the sample in order to obtain a range of  $q$  values. The  $\lambda$  of each detected neutron is calculated by time-of-flight.

The normalized reflected intensity ( $R$ ) is plotted against  $q$ . The  $R$ - $q$  curve results from the superposition of waves scattered by the interface. The amplitude and attenuation of each wave are determined by the thickness, roughness and scattering length density ( $\rho$ ) of each layer. Thickness and roughness represent structural information while  $\rho$  depends on the chemical composition and mass density,  $d$ :

$$\rho = d \frac{N_A}{M} \sum_{\text{molecule}} b_i \quad (2)$$

Download English Version:

<https://daneshyari.com/en/article/7895264>

Download Persian Version:

<https://daneshyari.com/article/7895264>

[Daneshyari.com](https://daneshyari.com)